

A South Pacific Cyclone-caused GPS Positioning Error and Its Impact on Remote Oceanic Island Communities

M. Filić

Sesvete, Zagreb, Croatia

R. Filjar

University of Rijeka, Rijeka, Croatia

Zagreb University of Applied Sciences, Zagreb, Croatia

ABSTRACT: Satellite navigation gains importance in sustainable development of modern civilisation. With the increasing number of GNSS-based technology and socio-economic systems and services, satellite navigation has become an essential component of national infrastructure. This calls for novel requirements on GNSS positioning performance, and increasing need for resilient GNSS development. Here we examined the impact of rapidly developing tropical cyclone on GPS positioning performance degradation, and the resulting impact on oceanic non-navigation and navigation GPS applications. We presented the methodology for indirect simulation-based GPS positioning performance evaluation through utilisation of experimental GPS observations, GNSS Software-Defined Radio (SDR) receiver, and a statistical analysis and framework we developed in the R environment for scientific computing. We identified alteration of GPS positioning error components time series statistical properties, and discuss the potential impact on GPS-based services essential for remote oceanic island communities. Manuscript concludes with the summary of findings, proposal for recommendations on improved GNSS resilience, and an outline for future research.

1 INTRODUCTION

Satellite navigation has become a foundation of modern civilisation and an indispensable component of the national infrastructure, regardless of the actual ownership of a satellite navigation system (UK Government Office for Science, 2018). As the result of a long-term trend, non-navigation applications of Global Navigation Satellite Systems (GNSS) overtook those navigation-related, facilitating the new perspective on GNSS positioning performance requirements. Smaller administrative regions with sparse population and the vast impact of the environment establish increasingly their socio-economic services on the utilisation of free-to-access and readily available satellite navigation services.

A remote oceanic island community provides an excellent example of the class (Howes, Birchenough, and Lincoln, 2018), (Yao, and Rhee, 2013). Facing growing challenges of climate change effects (The Economist, 2018), surrounded by the raising sea levels and extreme weather conditions, the investments in infrastructure shift to services based on low-cost maintenance and high efficiency infrastructure, such as GNSS. Increasing automation that provides a framework for sustainable community means increasing utilisation of GNSS. Considering this perspective, GNSS positioning performance gains new responsibility and requirements for stability and resilience against natural and artificial disturbances (Porreta *et al*, 2016).

Here we examine a case of a rapid tropical cyclone development in close proximity of a Pacific Ocean

island community from the perspective of GPS positioning performance degradation assessment, and potential impact on technology and socio-economic applications based on satellite navigation services.

2 METHOD

This section presents data and methods utilised in the study of troposphere-driven GPS positioning performance degradation.

2.1 Data description

International GNSS Service (IGS, 2018) provides a systematic access to archived GNSS-related daily observations collected by the IGS network (IGS, 2018) of stationary reference station spread across the Earth's surface. Provided on the voluntary basis as the service for scientists, researchers and practitioners, IGS reference stations differ in the range of observations they collect. Several of them deploy GPS-only dual frequency receivers, while the others gather observations from different GNSS systems simultaneously.

IGS network reference stations collect simultaneously several sets of observations (NASA, 2018), as follows: (i) dual frequency-GNSS pseudorange measurements (depending of the equipment used, GPS, GLONASS, Galileo, and Beidou) at 30 s sampling rate, (ii) navigation messages broadcast by related GNSS, (iii) (optional) addition observations of positioning environment, such as meteorological data at 15 min sampling rate, and (iv) (optional) observations of GNSS augmentation system information (WAAS, EGNOS etc.). Observations are structured in daily sets stored using a dedicated UNIX-based RINEX format, specified by (IGS et al, 2015), in related RINEX daily files (RINEX o and d files for GPS pseudorange measurements, RINEX n file for broadcast or received GPS navigation message etc.).



Figure 1. Noumea, New Caledonia (© OpenStreetMap contributors, (OpenStreetMap, 2018))

Data sets are freely available for individual (non-automated) access to scientists, researchers, practitioners and the other interested parties. On the common ground, the IGS network follow the same principle of data collection and storage that assures the quality of data. Primarily, the The IGS network has been set up to expose the impact of the GNSS ionospheric delay by not correcting the ionospheric effects in any way, while suppressing the other sources of GNSS pseudorange measurement errors. Still, a number of IGS reference station allow for contamination of the observed GNSS pseudoranges caused by the other sources of disturbance, such as tropospheric delay or satellite clock errors, to remain in records, thus allowing for research on the subject. We identified one source of GNSS pseudorange observations contaminated by uncorrected tropospheric delay in data collected at the IGS reference station in Noumea, New Caledonia (Figure 1), and used RINEX dual frequency GPS pseudorange measurements and RINEX navigation message files in this study.

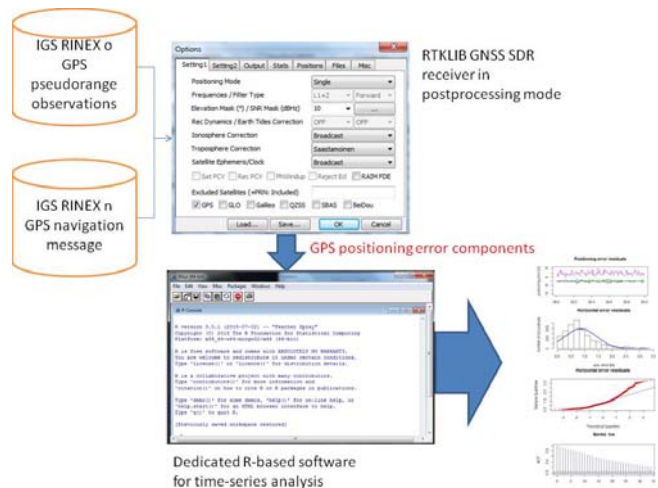


Figure 2. Data processing and analysis

2.2 Data processing and analysis

A procedure for data processing and analysis was used in the study, based on utilisation of a GNSS Software-Defined Radio (SDR) as a post-processing tool for position and positioning error estimation from RINEX data, and a dedicated statistical analysis software developed by our team in the open-source R framework for statistical computing (R project, 2018). Depicted in Figure 2, the procedure was established by our team and detailed elsewhere (Filic, Filjar, and Routsalainen, 2016). Essentially, it is a three-phase procedural that: (i) post-process experimental GNSS observations, corrupted with an error source under consideration (tropospheric effects, in this case), to yield time series of position vector and positioning error vector estimates; (ii) analyse GPS positioning error time series, and (iii) develop a model of GPS positioning error time series as the error residuals of the position estimation process. Our procedure allows for assessment of the GNSS positioning performance in various scenarios of applications and in different position environments through: (i) suitable configuration (switching off or on different pseudorange error correction models) of GNSS SDR

receiver utilised for processing, and (ii) selection of related GNSS observations sets at the IGS reference station position and the positioning environment conditions that corrupt the GNSS observations in a manner required for targeted study (Filić, Filjar, and Weng, 2018).

The first phase of the procedural utilised is based on Weighted Least-Square GPS position estimation process, as described elsewhere (Filić, and Filjar, 2018), (Oxley, 2017), (Filić, Grubišić, and Filjar, 2018). A comprehensive overview of mathematical foundations of the procedural's second and third phase is given in the remaining part of this section.

A linear additive GPS positioning error model is assumed, in a form presented with Eq (1).

$$\vec{\hat{x}} = \vec{x} + \delta\vec{x}_{iono} + \delta\vec{x}_{tropo} + \delta\vec{x}_{sat-clock} + \delta\vec{x}_{sat-ephem} + \vec{\epsilon} \quad (1)$$

where:

$\vec{\hat{x}}$... GPS-based position estimate, contaminated with effects of error sources
 \vec{x} ... real (true) position
 $\delta\vec{x}_{iono}$... position estimation error vector, due to ionospheric effects
 $\delta\vec{x}_{tropo}$... position estimation error vector, due to tropospheric effects
 $\delta\vec{x}_{sat-clock}$... position estimation error vector, due to satellite clocks error effects
 $\delta\vec{x}_{sat-ephem}$... position estimation error vector, due to satellite position estimation error effects
 $\vec{\epsilon}$... residual position estimation vector, due to causes un-accounted for in previous position estimation error vectors

Suppose the means exist for removal entirely of the position estimation error, due to tropospheric effects. In that case, the GPS-based position estimate would comprise all the other effects, but without the tropospheric one, and be expressed as in Eq (2).

$$\vec{\hat{x}}_{-t} = \vec{x} + \delta\vec{x}_{iono} + \delta\vec{x}_{sat-clock} + \delta\vec{x}_{sat-ephem} + \epsilon \quad (2)$$

Assuming the position estimates derived from (1) and (2), respectively, are known, the GPS positioning error, due to tropospheric effects, may be determined using the model (3).

$$\delta\vec{x}_{tropo} = \vec{\hat{x}} - \vec{\hat{x}}_{-t} \quad (3)$$

We created a time series of tropo-free GPS-based position estimates time series (2) by introduction of Saastamoinen tropospheric delay correction (Parkinson, and Spilker Jr, 1996) during post-processing RINEX observation with RTKLIB GNSS SDR receiver. Saastamoinen developed an empirical model valid for satellite signals approaching the GPS receiver aerial at elevation angles higher than 10°, as given with Eqs (4), (5) and (6).

$$d_{tropo} [m] = 0.002277(1+D)sec\psi_0 \left[P_0 + \left(\frac{1255}{T_0} + 0.005 \right) e_0 - B \tan^2 \psi_0 \right] + \delta_R \quad (4)$$

where:

$$D = 0.0026 \cos 2\phi + 0.00028h \quad (5)$$

ϕ ... denotes latitude of a GPS receiver
 h ... denotes height above the mean sea level of the GPS receiver's position, in [m]
 P_0 ... denotes atmospheric pressure in [hPa]
 e_0 ... denotes partial water vapour pressure in [hPa]
 T_0 ... denotes air temperature in [K]

$$\psi_0 = 90^\circ - E \quad (6)$$

E ... denotes elevation angle of satellite signal approach in [°]
 B, δ_R ... two height-dependant correction terms (Parkinson, and Spilker, Jr, 1996)

All the vectors listed in Eqs (1), (2), and (3) may be expressed with the related three independent components from the end user's perspective, as defined by Eq (7).

$$\vec{x}_i = x_{northing-i} \cdot \vec{i} + x_{easting-i} \cdot \vec{j} + x_{vertical-i} \cdot \vec{k} \quad (7)$$

where:

x_i ... a vector from (1)
 $x_{northing-i}$... northing component of \vec{x}_i
 $x_{easting-i}$... easting component of \vec{x}_i
 $x_{vertical-i}$... vertical component of \vec{x}_i
 $(\vec{i}, \vec{j}, \vec{k})$... a set of unit vectors for definition of the northing, easting and vertical directions, respectively, according to World Geodetic System 1984 (Eurocontrol, 1998)

Components of the GPS positioning error vector, due to tropospheric effects, (3) may be presented in the manner of (7) with Eq (8).

$$\delta\vec{x}_{tropo} = x_{northing-tropo} \cdot \vec{i} + x_{easting-tropo} \cdot \vec{j} + x_{vertical-tropo} \cdot \vec{k} \quad (8)$$

The horizontal component of the GPS positioning error vector, due to tropospheric effects, may be determined as the combination of the GPS northing and easting positioning error components, as in Eq (9).

$$x_{horizontal-tropo} = \sqrt{x_{northing-tropo}^2 + x_{easting-tropo}^2} \quad (9)$$

Eqs (8) and (9) define time-series of the GPS northing, easting, vertical and horizontal time series, respectively. Characterisation of time-series may be performed using a procedure involving: (i) the time-series mean and standard deviation values determination, (ii) residual statistical distribution, or (Gaussian) kernel density analysis, (iii) the Quantile-Quantile (Q-Q) diagram analysis, (iv) Partial Auto-Correlation Function (PACF) analysis, and (v) residual error Auto-Regressive (AR) model development.

The Kernel density estimation method is defined as follows. Let (10) be a time series of the population samples with the unknown distribution f . The f distribution may be estimated using kernel density estimator (11).

$$(x_1, x_2, \dots, x_n) \quad (10)$$

$$\widehat{f}_h(x) = \frac{1}{n} \sum_{i=1}^n K_h(x - x_i) = \frac{1}{nh} \sum_{k=1}^n K\left(\frac{x - x_i}{h}\right) \quad (11)$$

with:

K ... Gaussian kernel (non-negative integrable function) $K(u) = \frac{1}{\sqrt{2\pi}} e^{-\frac{u^2}{2}}$
 h ... bandwidth (smoothing parameter)

Bandwidth h is defined in the optimal manner that minimises the mean integrated square error, with the resulting optimised model given with (12).

$$h = \left(\frac{4 \cdot \widehat{\sigma}^5}{3 \cdot n} \right)^{\frac{1}{5}} \approx 1.06 \cdot \widehat{\sigma} \cdot n^{-\frac{1}{5}} \quad (12)$$

The Quantile-Quantile (Q-Q) diagram is a graphical method for comparison between two statistical distribution by plotting their quantiles against each other (Shumway, and Stoffer, 2017).

The Partial Auto-Correlation Function (PACF) is defined (Box, Jenkins, and Reinsel, 2008) as follows. Let z_t denotes a given time series of samples. The PACF is defined as a set of partial auto-correlation coefficients of lag k , defined as the auto-correlation between z_t and z_{t+k} with lags larger than 1 and less or equal to $k-1$ not included (13), (14).

$$\alpha(1) = \text{Corr}(z_{t+1}, z_t) \quad (13)$$

$$\alpha(k) = \text{Cor}(z_{t+k} - P_{t,k}(z_{t+k}), z_t - P_{t,k}(z_t)) \quad (14)$$

where $P_{t,k}$ refers to projection of x to space determined by $xt+1, \dots, xt+k-1$.

The GPS positioning errors, due to tropospheric effects, time series under observation were considered time series of residuals, and characterised using Auto-Regressive (AR) models of random processes. An AR model of order p is of the form expressed with Eq (15).

$$x(t) = c + \sum_{i=1}^p \phi_i x_{t-i} + \epsilon_t \quad (15)$$

where:

$\phi_1, \phi_2, \dots, \phi_p$... denote a set of the model parameters
 c ... denotes a constant (bias)
 ϵ_t ... denotes white noise model error

AR model and the methodology for its parameters determination are discussed elsewhere, for instance (Shumway, and Stoffer, 2017).

The methods and algorithms presented in this Section were deployed in the R programming framework for statistical computing (R project team,

2018), and assembled into the dedicated time series analysis framework by our team.

3 CASE STUDY DESCRIPTION

A case study of a rapid development of a tropical cyclone in a close vicinity to the observation (IGS reference station Noumea, New Caledonia in South Pacific) site was selected, as a case of both an extreme (tropospheric) positioning environment condition, and of real situation encountered by remote oceanic island community. The severe tropical cyclone Ola developed on 29th January, 2015 (DOY029) far in the north to north-west direction from the Noumea reference station. Ola progressed in southern direction, reaching the closest point to New Caledonia on 30th January, 2015, finally disintegrating on 3rd February, 2015. In its peak intensity, Ola reached the Category 3 severe tropical cyclone strength (Australian scale) on DOY030, with winds at 150 km/h and barometric pressure of 955 hPa at its peak intensity (Storm Science Australia, 2018).

The extreme (tropospheric) weather conditions in rapid developments cause considerable impact on GPS pseudorange measurement by introduction of random tropospheric delay (Parkinson, and Spilker, Jr, 1996). The case of Ola's peak intensity taking place close to the IGS reference station in New Caledonia was examined in this study for potential effects on GPS positioning performance with repercussions on GPS-based applications.

4 STUDY RESULTS

Obtained during the implementation of data processing and analysis procedure, outlined in Section 2.2, are presented in this Section, as follows.

Tables 1 and 2 show the mean and standard deviation values of the GPS positioning error components, due to tropospheric effects, on the days 028 and 030 in 2015, respectively.

Table 1. Mean values of GPS positioning error components, due to tropospheric effects

Residual mean values	DOY028	DOY030
Northing error [m]	-0.309	-0.307
Easting error [m]	-0.017	-0.009
Horizontal error [m]	0.436	0.855
Vertical error [m]	9.351	9.188

Table 2. Standard deviation values of GPS positioning error components, due to tropospheric effects

Residual standard deviation	DOY028	DOY030
Northing error [m]	0.857	0.851
Easting error [m]	0.525	0.502
Horizontal error [m]	0.750	0.582
Vertical error [m]	1.836	1.824

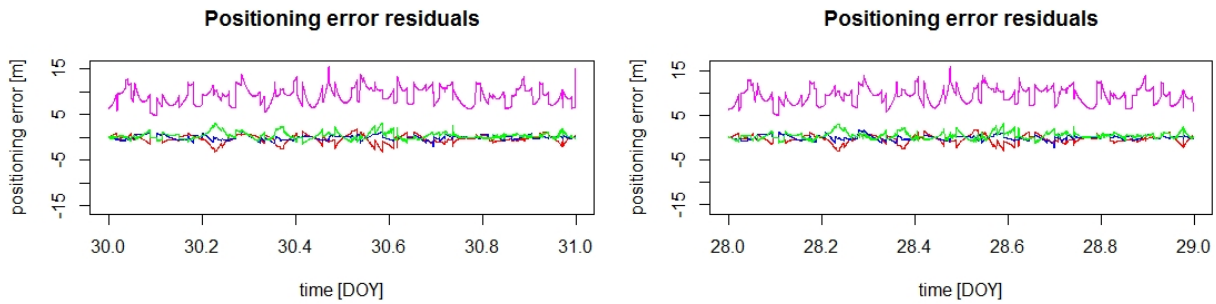


Figure 3. Time series of GPS northing (red), easting (blue), horizontal (green), and vertical (magenta) positioning errors, on DOY028 (left) and DOY030 (right), respectively.

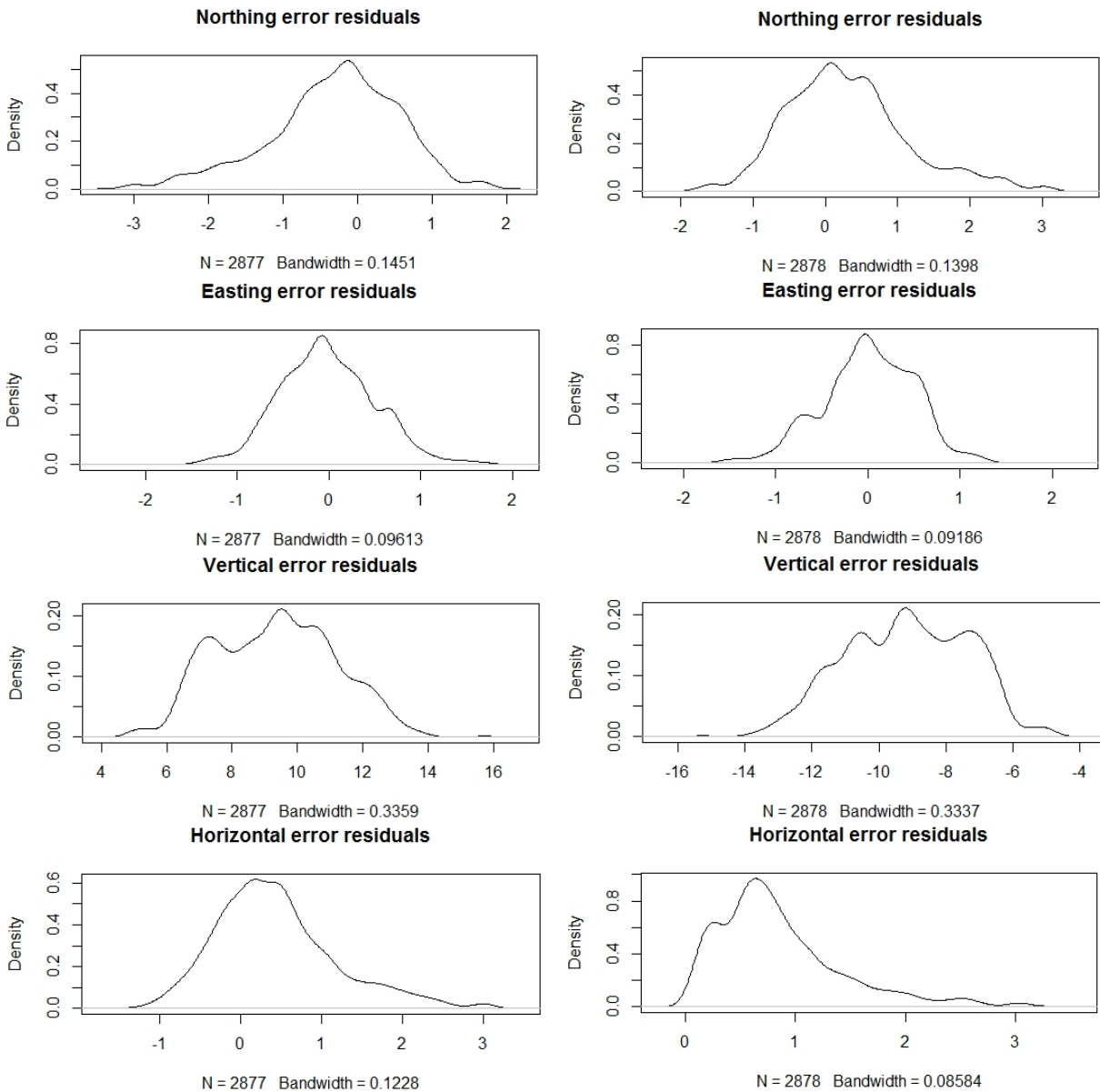


Figure 4. Estimated statistical kernel densities of GPS northing, easting, vertical and horizontal positioning errors, respectively, on DOY028 (left) and DOY030 (right).

Time series of northing, easting, horizontal, and vertical positioning error components, due to tropospheric effects, on days 028 (quiet weather) and 030 (the full extent of a tropical cyclone) in 2015 are depicted with combined diagrams in Figure 3.

Kernel density estimates of the northing, easting, horizontal, and vertical GPS positioning error

components on the days 028 and 030 in 2015 are depicted in Figure 4.

Q-Q diagrams of the northing, easting, horizontal, and vertical GPS positioning error components for the days 028 and 030 in 2015 are depicted in Figure 5.

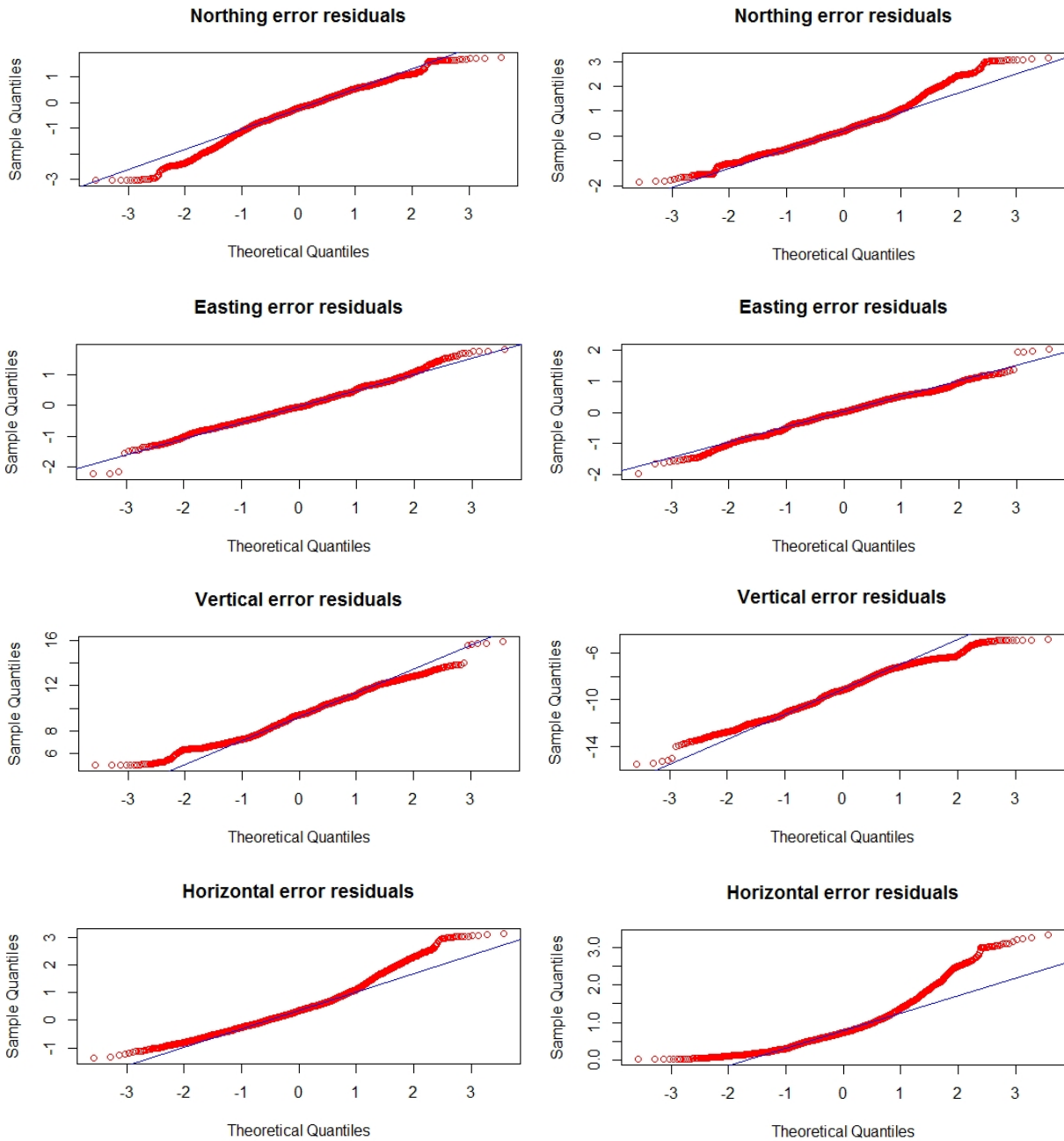


Figure 5. Q-Q plots of GPS northing, easting, vertical, and horizontal positioning errors time series, respectively

Partial Auto-Correlation Function diagrams of the northing, easting, horizontal, and vertical GPS positioning error components for the days 028 and 030 in 2015 are depicted in Figure 6.

Finally, summary of Auto-Regressive (AR) models (mean and variance values) for the northing, easting, horizontal, and vertical GPS positioning error components are outlined in Tables 3 and 4, respectively.

Table 3. Auto-Regressive (AR) model means for the northing, easting, horizontal and vertical GPS positioning error components on the days 028 and 030 in 2015

AR model mean	DOY028	DOY030
Northing error [m]	-0.3091199	-0.3068283
Easting error [m]	-0.01667184	-0.009313357
Horizontal error [m]	0.4359185	0.854925
Vertical error [m]	9.351068	9.187918

Table 4. Auto-Regressive (AR) model variations for the northing, easting, horizontal and vertical GPS positioning error components on the days 028 and 030 in 2015

AR model σ^2	DOY028	DOY030
Northing error [m]	0.0315	0.02935
Easting error [m]	0.02155	0.01846
Horizontal error [m]	0.05241	0.02472
Vertical error [m]	0.2326	0.2605

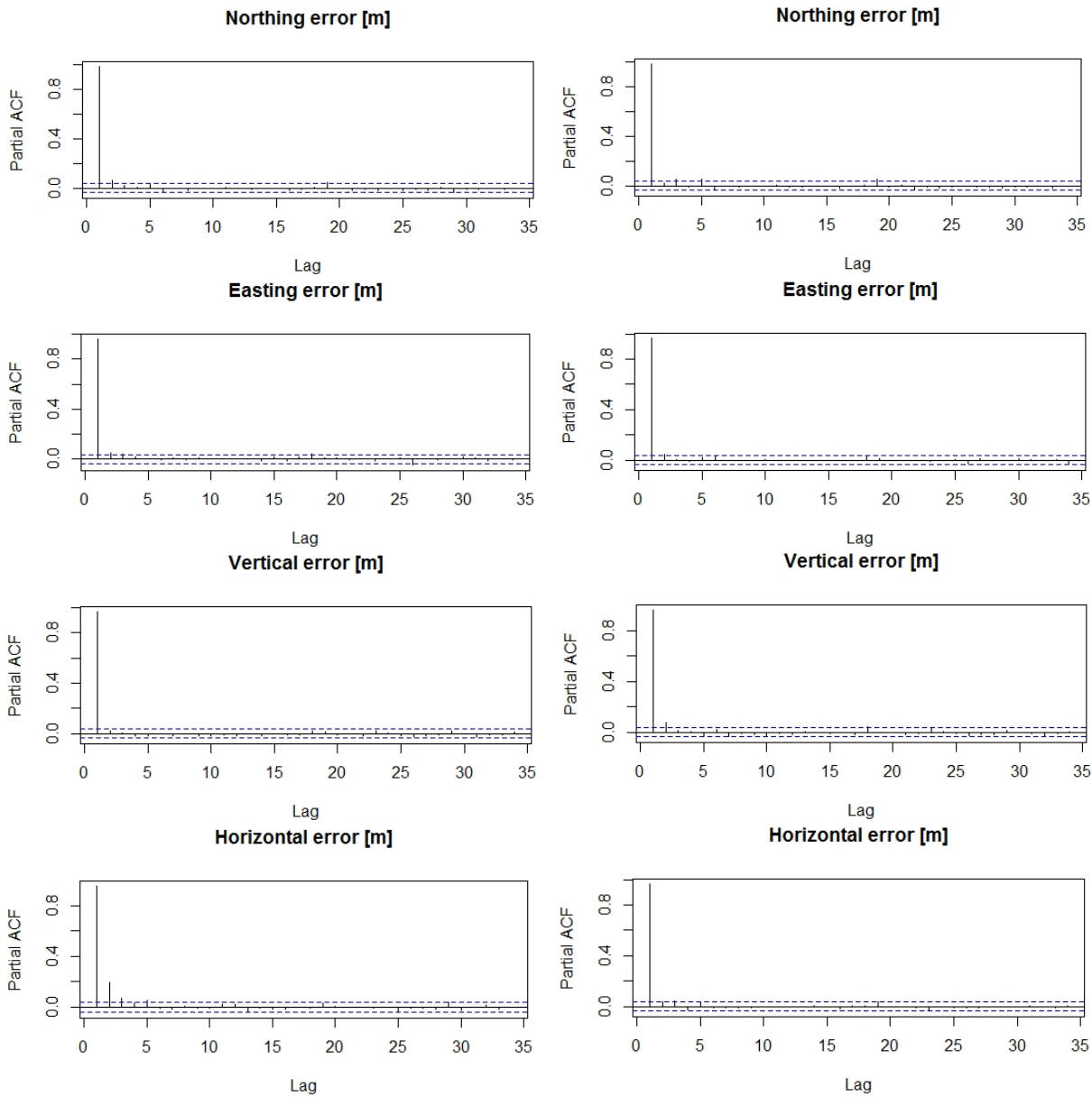


Figure 6.

5 DISCUSSION AND CONCLUSION

The GPS position estimation accuracy is the GPS positioning performance index largely affected by introduction of tropospheric delay. The statistical properties of tropospheric delay guides the selection of approach in error correction model development. The over-all position estimation error due to tropospheric effects determines the GPS suitability for robust and resilient GPS-based applications development and operation.

Mean and standard deviation values (Table 1 and 2, respectively) of GPS positioning error components time series (Figure 3) do not reveal a substantial difference between quiet tropospheric conditions and a tropical cyclone. This may be understood the result of dominance of dry-air component of tropospheric delay. However, it is the wet-air component of tropospheric delay that delivers variation in time series, with its increasing impact during the time of a tropical cyclone. Estimates of kernel density (Figure 4) for the cases of quiet atmosphere and a tropical cyclone shows evident differences, with the only

exception of easting GPS positioning error component, that remained in following the normal-like statistical distribution. The findings were confirmed with Q-Q diagrams for related GPS positioning error components (Figure 5), were again the eastern GPS positioning error component produced the normal-like distribution plots for both quiet and disturbed atmosphere. Further examination of Partial Auto-Correlation Function (PACF) diagrams revealed low variations of all GPS positioning error components in quiet atmospheric conditions, without auto-correlation coefficients exceeding the confidence bounds. Tropical cyclone conditions altered dynamics of all, but the easting GPS positioning error components, adding several auto-correlation coefficients that exceeded the confidence bounds, making the case of introduction of AR(2) model as a suitable one capable of taking the newly introduced variability into account.

In summary, we accentuated the impact of tropospheric delay on GPS positioning performance through assessment of the case of rapid and extreme tropospheric weather deterioration. The evidence

shows different nature of troposphere-driven GPS positioning error during a tropical cyclone, compared with the case of quiet tropospheric weather. While essential statistical parameters of GPS positioning error components remain balanced and stable regardless of tropospheric conditions, statistical properties of GPS positioning error components vary largely in relation to the nature and intensity of tropospheric disturbance. Different nature of tropospheric delay (i. e. tropospheric contribution to GPS pseudorange measurement error) reflects on the over-all GPS positioning accuracy (Filić, Filjar, 2018). Deterioration may not affect oceanic cruise navigation, due to its low requirements on position estimation accuracy, but impacts significantly performance of numerous technology and socio-economic GPS-relying services for remote oceanic island communities. With restricted budget for expensive infrastructure, those communities utilise satellite navigation extensively. Thus, any impact on stability and reliability of GPS-based services may undermine communities already facing challenges of climate change, and potential devastating impact on community's survival. Considering results of this study, recommendations may be proposed on: (i) continuous observations of meteorological parameters related to GPS positioning performance, (ii) timely delivery of meteorological observation parameters to GPS receivers for more effective tropospheric error mitigation; and (iii) continuous research on user equipment adaptation to positioning environment dynamics in a sense of intelligent mitigation of the effects of potential disruptions.

We intend to continue our research on the subject through examination of cases with transitional periods between extreme conditions, and their impact on GPS tropospheric delay and GPS positioning error dynamics in continuous aim to develop an adaptive positioning estimation model capable of detecting anomalies in positioning environment and responding to their mitigation without affecting the GNSS positioning performance and quality of GNSS-based applications.

REFERENCE

- Box, G E P, Jenkins, G, and Reinsel, G C. (2008). *Time Series Analysis, Forecasting and Control* (4th ed). John Wiley & Sons. Hoboken, NJ.
- Filić, M. (2018). On development of the forecasting model of GNSS positioning performance degradation due to space weather and ionospheric conditions. *Proc 2nd URSI AT-RASC* (4 pages, electronic format). Gran Canaria, Spain. Available at: <http://www.atrasc.com/content/stick/papers/URSISummaryPaperMFilic.pdf>
- Filić, M, and Filjar, R. (2018). Forecasting model of space weather-driven GNSS positioning performance. Lambert Academic Publishing, Riga, Latvia.
- Filić, M, Grubišić, L, and Filjar, R. (2018). Improvement of standard GPS position estimation algorithm through utilization of Weighted Least-Square approach. *Proc of 11th Annual Baška GNSS Conference*, 7-19. Baška, Krk Island, Croatia. Available at: <https://www.pfri.uniri.hr/web/hr/dokumenti/zbornici-gnss/2018-GNSS-11.pdf>
- Filić, M, Filjar, R, Weng, J. (2018). An IGS-based simulator of ionospheric conditions for GNSS positioning quality assessment. *Coordinates*, 14(1), 31-34. Available at: <http://mycoordinates.org/an-igs-based-simulator-of-ionospheric-conditions-for-gnss-positioning-quality-assessment/>
- Filić, M, Filjar, R, and Ruotsalainen, L. (2016). An SDR-based Study of Multi-GNSS Positioning Performance During Fast-developing Space Weather Storm. *TransNav*, 10, 395-400. doi: 10.12716/1001.10.03.03. Available at: <http://bit.ly/2fxAvph>.
- Howes E L, Birchenough, S, and Lincoln, S. (2018). Effects of Climate Change Relevant to the Pacific Islands (in Pacific Marine Climate Change Report Card). Commonwealath Marine Economies Programme (Funded by HM Government of the United Kingdom). London, UK. Available at: <https://bit.ly/2qdI2gZ> (HM Government of the UK internet resource).
- IGS. (2018). International GNSS Service (IGS) Network. Available at: <http://www.igs.org/network>
- IGS, RINEX Working Group, and RTCM-SC104. (2015). RINEX: The Receiver Independent Exchange Format (version 3.03). Available at: <ftp://igs.org/pub/data/format/rinex303.pdf>
- NASA. (2018). IGS Archive of daily GNSS observations, hosted by NASA. Available at: <ftp://cddis.gsfc.nasa.gov/gnss/data/daily>
- OpenStreetMap. (2018). Data base of world spatial data under Open Database Licence. Cartography provided under the Creative Commons Attribution-ShareAlike 2.0 license. Available at: <https://www.openstreetmap.org>
- Oxley, A. (2017). *Uncertainties in GPS Positioning: A mathematical discourse*. Academic Press/Elsevier. London, UK.
- Parkinson, B W, and Spilker, Jr, J J (eds). (1996). *Global Positioning System: Theory and Applications* (Vol. I). AIAA. Washington, DC.
- Porretta, M et al. (2016): GNSS Evolutions for Maritime: An Incremental Approach. *Inside GNSS*, May/June, 2016, 54-62. Available at: <http://insidegnss.com/auto/mayjune16-WP.pdf>
- R-project team. (2017). *The R project for Statistical Computing* (software, documentation, and books). Available at: <https://www.r-project.org>.
- Shumway, R H, and Stoffer, D S. (2017). *Time Series Analysis and Its Applications With R Examples* (Fourth Edition). Springer Verlag. Cham, Switzerland. Available at: <https://www.stat.pitt.edu/stoffer/tsa4/tsa4.pdf>
- Storm Science Australia. (2018). Tropical Cyclone Ola in the Eastern Coral Sea. *Storm Science Australia*. Available at: <http://bit.ly/2BJkunk>
- Stull, R. (2017). *Practical Meteorology: An Algebra-based Survey of Atmospheric Science* (version 1.02b). Univ. of British Columbia. Vancouver, BC. Available at: <https://bit.ly/2QXfG66>
- Takasu, T. (2013). RTKLIB: An Open Source Program Package for GNSS Positioning. Software and documentation available at: <http://www.rtklib.com>
- The Economist. (2018). Stormy Weather: Storms in America and the Pacific are evidence of climate change. *The Economist UK ed*, Sep 22, 2018, 52-54. Available at: <https://econ.st/2MPZwZj>
- Thomas, M et al. (2011). *Global Navigation Space Systems: reliance and vulnerabilities*. Royal Academy of Engineering. London, UK. Available at: <http://bit.ly/1vrIenu>
- UK Government Office for Science. (2018). *Satellite-Derived Time and Position: A Study of Critical Dependencies*. HM Government of the UK and NI. Available at: <https://bit.ly/2E2STnd>
- Eurocontrol, and IfEN. (1998). *WGS 84 Implementation Manual*. Available at: <http://bit.ly/2wM4xPn>
- Yao, X, and Rhee, C. (2013). *The economics of climate change in the Pacific*. Asian Development Bank. Mandaluyong City, Philippines. Available at: <https://bit.ly/2pcpCi9>